Comparison of experimental and simulated $K\alpha$ yield for 400 nm ultrashort pulse laser irradiation

F. Y. Khattak, O. A. M. B. Percie du Sert, and D. Riley
School of Mathematics and Physics, Queen's University of Belfast, University Road, Belfast BT7 1NN, United Kingdom

P. S. Foster, E. J. Divall, C. J. Hooker, A. J. Langley, and J. Smith
Central Laser Facility, CLRC Rutherford Appleton Laboratory, Chilton, Didcot, Oxon OX11 0QX, United Kingdom

P. Gibbon
John von Neumann Institute for Computing, Central Institute for Applied Mathematics (ZAM), Computer Simulations Division, Research Centre Jülich, D-52425 Jülich, Germany

(Received 15 March 2006; published 29 August 2006)

Ti $K\alpha$ emission yields from foils irradiated with ~45 fs, p-polarized pulses of a frequency-doubled Ti:sapphire laser are presented. A simple model invoking vacuum heating to predict absorption and hot electron temperature was coupled with the cross section for K-shell ionization of Ti and the Bethe-Bloch stopping power equation for electrons. The peak predicted $K\alpha$ emission was in generally good agreement with experiment. This contrasts strongly with previous work at the fundamental frequency. Similar predictions using particle-in-cell (PIC) code simulation to estimate the number and temperature of hot electrons also gave good agreement for yield.

DOI: 10.1103/PhysRevE.74.027401 PACS number(s): 52.38.Ph, 52.38.Dx, 52.70.La

I. INTRODUCTION

The study of $K\alpha$ emission from ultrashort pulse laser-produced plasmas has been pursued by several groups [1–13]. Such studies give clues to the propagation of fast electrons in different types of solids as well as the plasma conditions created [14]. This may be important in the development of fast ignitor fusion and fast x-ray sources for a variety of applications [15], such as ultrafast diffraction and probing.

Using fundamental laser radiation, usually at 800 nm, experiments on a variety of target materials with pulses from 30–200 fs [1–15] have shown typical $K\alpha$ conversion efficiencies in the range 10^{-6}–10^{-4}. The generation of $K\alpha$ photons is governed by two principal issues. Firstly, there is the interaction of the laser with the target—usually with a substantial preformed plume. This determines the number and energy of the fast electrons. Then there is the transport of the fast electrons into the foil where they ionize cold atoms and generate $K\alpha$ emission. Models that treat either of these issues are available [16–19]. However, models that treat both together are not yet available and in general it has proved hard to reproduce experimental yields with simple modeling. In this paper we show that when using frequency-doubled pulses to avoid the preplasma production, we are able to get good agreement for the maximum $K\alpha$ yield with relatively simple models.

II. EXPERIMENTAL SETUP AND DATA

The experimental arrangement has been presented previously [20]. The ASTRA Ti:sapphire laser was used in second harmonic, by use of a KDP type-I crystal which was 0.6 mm thick and allowed up to 60 mJ of 400 nm light on target per shot. The 400 nm beam was reflected off three dielectric mirrors, effectively rejecting the unconverted amplified spontaneous emission (ASE) prelase and prepulses. After reflection from a Ag mirror, the beam was focussed onto target by a Ag-coated off-axis parabola (OAP) in an $f/2.5$ cone. Leakage of 400 nm light through the second dielectric was used to monitor the energy of the blue beam via a photodiode coupled to an integrating sphere with IR filtering to cut out 800 nm light.

The focal spot was measured at the focal position in the chamber with an objective coupled to an 8-bit charge-coupled device (CCD) with the fundamental beam attenuated to 1% of maximum at the input to the compressor using a waveplate. At best focus typically 35% of the light was contained in the central spot which was only 1.5 μm $\times$ 1.9 μm full width at half maximum (FWHM). At larger offsets the focal spot contained several small hot spots and the total energy was contained within the spot determined by geometrical optics.

The principal diagnostic was a time-integrating von Hamos spectrometer consisting of a LiF (200) crystal and a 16-bit CCD detector. This instrument has been previously calibrated at 5.9 keV [9] and since, in theory, the reflectivity does not vary much between 4.5 and 5.9 keV we used a scaled value in our data analysis. We also used an Axis Photonique x-ray streak camera with a KI photcathode to achieve ~0.7 ps resolution, which looked directly at the target. Ti and Sc filtering was used across the slit to show that with 12.5 μm Ti filter, the camera was sensitive primarily to the $K\alpha$ and He α lines with the former being dominant away from best focus. We were able to look at both s and p polarization by rotating the targets in the appropriate planes. For p-polarized light we measured the specular reflection from the targets using a Molectron energy monitor—we were not equipped to make measurements of the nonspecular scatter.

Figure 1 illustrates the principal results. In Fig. 1(a) we see the $K\alpha$ emission for p polarization at 3 angles of inci-

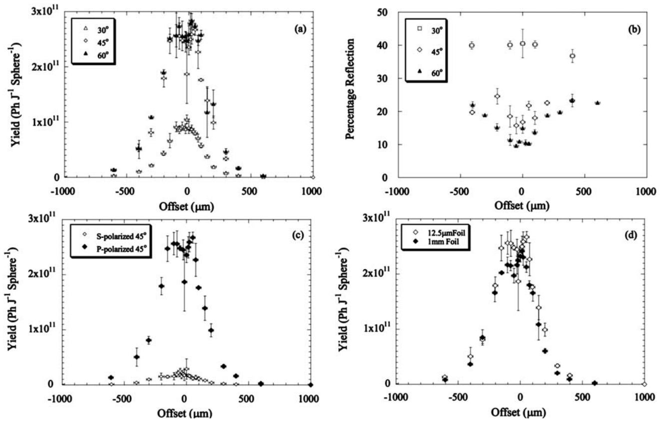

FIG. 1. (a) $K\alpha$ yield for 12.5-μm-thick foils with p-polarization at different angles of incidence. Positive offset means the focus is behind the target. (b) Specular reflectivity for similar targets under similar irradiance conditions. (c) Comparison of the $K\alpha$ yield for s and p polarization for the same conditions as (a) for 45° incidence. (d) Comparison of the $K\alpha$ yield for 12.5-μm- and 1-mm-thick targets; note the slightly higher yield for the thinner targets. In all cases the data are an average of at least five data shots with the standard deviations being represented by the error bars. The error bar in the offset is $\sim\pm 10$ μm.

dence. We see that there is a significant increase after 30° but after 45° the increase is somewhat smaller. This is mirrored in the measured specular reflectivity seen in Fig. 1(b). In Fig. 1(c) we compare S and P polarization for 45°. Clearly, there is a strong difference and that even at tight focus the polarization appears well defined. In Fig. 1(d) we compare the $K\alpha$ emission at 45° for a 12.5-μm-thick target with that for a 1 -mm-thick Ti target. The thicker target has slightly less emission than the thinner foil, rather than slightly more as might be expected.

III. MODELING

We model the $K\alpha$ emission in our data with a simple approach. Firstly, we use the Brunel vacuum heating model [21] to calculate both the hot electron temperature ($T_{\rm hot}$) and absorption fraction, as shown in Fig. 2. This assumes a prepulse free laser-solid interaction. For the second harmonic we expect this to be a reasonable assumption and the strong dependence of both the $K\alpha$ yield and specular reflectivity on the angle of incidence supports this assertion.

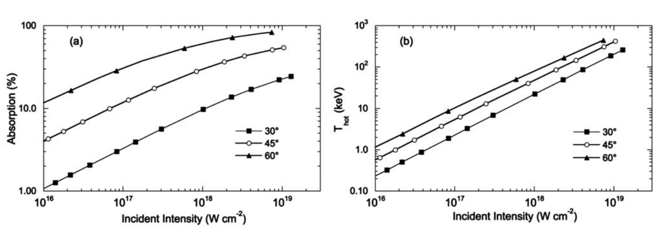

FIG. 2. Parameters from the Brunel vacuum heating model for 400 nm incidence with p polarization. The high absorption predicted for the 60° incidence case is likely to be an overestimate as discussed in the text.

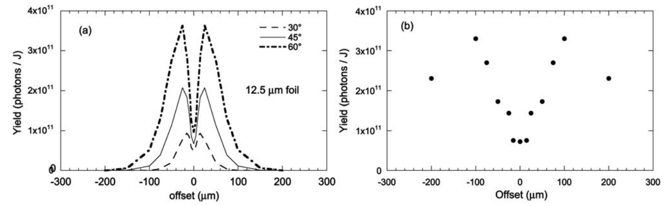

FIG. 3. (a) Simulated yield of $K\alpha$ photons for a 12.5 μm foil for three angles of incidence. Note the good agreement with experiment [Fig. 1(a)] for peak yield for the 30° and 45° cases. In each case, the contribution of the low intensity "halo" at tight focus is not counted and will have the effect of filling in the dip. (b) Simulated yield obtained using the BOPS PIC code to obtain both the number and temperature of hot electrons.

Next, we assume a Maxwellian distribution [2] with a temperature $T_{\rm hot}$. We calculate the number of electrons in 112 equally spaced energy bins out to energy 5.6 k $T_{\rm hot}$. We divide the foil into cells of $10^{-2}\mu$m and for each energy group we transport the electrons through the cells using the relativistic ionization cross section [22] to calculate the $K\alpha$ photons generated. For each ionization event, an electron is lost from the beam. The reabsorption of the $K\alpha$ photons is accounted for according to the depth of the cell in the foil. Slowing of the electrons via collisions is included via the Bethe stopping formula [23]. Once an electron group emerges from the rear of the foil it is assumed to play no further role.

Figure 3(a) shows results for a 12.5 μm foil. Note that the peak value of emission is in good agreement with experiment for 30° and is about 25% lower and 40% higher than experiment for 45° and 60°, respectively. This last result might be explained by saturation of absorption in vacuum heating. It has been shown by Brunel [24] that the vacuum heating model will overestimate the level of absorption at high intensity, as it neglects the $\mathbf{v}\times\mathbf{B}$ force. Given the high level of absorption predicted for a 60° incidence, there is a strong possibility that it is overestimated. Note also that there is a stronger dip at tight focus than seen experimentally. This is to be expected since the tight focus has only 35% of energy in the central peak and there is a halo of lower irradiance ($\sim 8\times 10^{17}$ W cm^{-2} that contains $\sim$45% of energy with the rest spread over a larger area). The averaging of irradiance will fill in the central dip to a large degree. Averaging again may play a role in our third observation: that the predicted width of the emission with offset is $\sim$100 μm in contrast to $\sim$400 μm experimentally. Moving away from best focus, the focus will develop "hot spots" that will enhance emission locally and thus may contribute to a broadening effect in the yield versus the offset curve.

For the 60° case we used the BOPS PIC code [25] to simulate absorption and $T_{\rm hot}$ for a limited set of offsets. The code uses up to 25 000 cells and 0.5×10^6 particles and takes several hours per run. We do indeed find that at the peak irradiance absorption drops to $\sim$13% with $T_{\rm hot}\sim$210 keV. Figure 3(b) shows the predicted $K\alpha$ yield for different offsets when we use the PIC code to determine the number and temperature of fast electrons. It appears that despite the different absorption, the predicted peak yields are similar to the Brunel predictions, perhaps because $T_{\rm hot}$ is lower and fewer

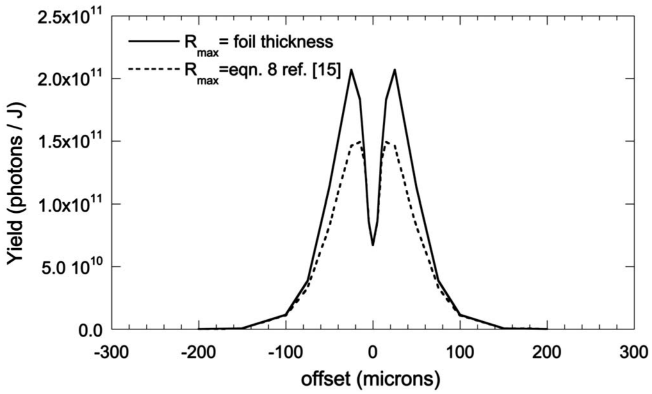

FIG. 4. Comparison of simulations with the Brunel model, for thick and thin foils. There only a slight increase for thick foils as the $K\alpha$ photons originating deeper than $\sim 20\ \mu$m are reabsorbed.

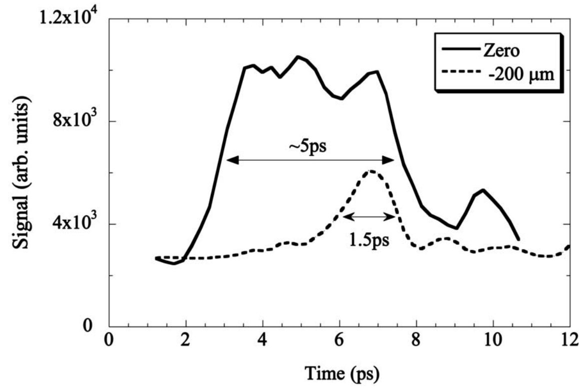

FIG. 5. Streak line outs taken with an Axis Photonique camera. The x rays illuminated the slit directly and the use of two filters of Ti and Sc and comparison with the time integrated spectra allowed us to confirm that the contributions from the $K\alpha$ emission dominate the signal.

electrons are predicted to pass through the foil without interacting. One difference is that the PIC code seems to predict higher absorption out to high offset and would thus predict a higher width of the peak with offset—in better agreement with experiment. This behavior, coupled with the low absorption at tight focus seems to conflict with the experimental specular reflectivity data. It may be that at tight focus, there is significant nonspecular reflection. We also note that for the high offsets, we expect $T_{\rm hot} \sim$ few keV, whereas the initial temperature must be ~ 1 keV to resolve the Debye length and PIC simulations with low $I\lambda^2$ at higher offsets than shown are not so reliable.

In Fig. 4 we compare 12.5 μm and 1 mm foils from our model based on vacuum heating. The thicker foil has slightly more emission due to having more material for the electrons to interact with: it is only slightly higher because the absorption length of the $K\alpha$ photons is only $\sim 20\ \mu$m, so much of the 1 mm foil does not contribute to the signal. Experimentally [see Fig. 1(d)], the situation is reversed, with the thinner foil being more efficient close to tight focus. We surmise from this that fast electrons are indeed able to penetrate the thinner, foil. As they exit, they are pulled back into the foil and make a further contribution to the $K\alpha$ signal. In the 1 mm foil, these electrons mainly penetrate too deeply to contribute to the $K\alpha$ signal.

So far we have made no reference to the time scale on which the electrons penetrate the foil. As pointed out by Bell *et al.* [17], if we assume this happens on the time scale of the laser pulse, the predicted current would generate an energetically impossible magnetic field. What is expected is that the electrons would be confined by a large electric field to the surface plasma until a cold return current neutralized the fast electron current. The time scale for this should depend on the resistivity of the target. X-ray streak data from the foils, as shown in Fig. 5, showed $K\alpha$ pulse durations ranging from ~ 1.5 to ~ 5 ps, indicating that this is the time scale on which fast electrons penetrate the foil. The penetration depth of the electrons is expected to be affected by the self-generation of magnetic and electric fields.

Using Eq. (8) of Bell *et al.* [17] together with the cold conductivity of Ti ($\sim 2.4 \times 10^6\ \Omega^{-1}\,\mathrm{m}^{-1}$), we estimate the maximum range to be $\sim 23\ \mu$m for tight focus, which exceeds the thin foil width. For large focal offsets, with their lower value of $T_{\rm hot}$, the penetration depth starts to be less than the foil width, but the Bethe-Bloch stopping distance also drops. In fact, it is for the intermediate regime of $\sim 25-50\ \mu$m offset that the predicted penetration depth is smaller than both the foil thickness and the Bethe-Bloch stopping range.

If we redo our calculation taking the penetration depth given by Bell *et al.* as the foil thickness where this is less than the actual foil depth then we get a yield of $\sim 1.5 \times 10^{11}$ photons/J, still quite close to the experimental value. Comparing Figs. 1(d) and 4 we estimate that $\sim 30\%$ of the signal close to tight focus comes from recirculated electrons coming back after exiting the foil. This would then fill in the central dip and bring the yield back close to the experimental value. We should also consider the slowing of the electrons as they penetrate the foil due to the retarding electric field. This effect would change the cross section for ionization. However, the cross section varies by less than a factor of 2, for example, between 0.1 and 10 MeV, the regime of interest for close to tight focus.

The above arguments assume the conductivity of the Ti is not much changed by fast electron heating. We can make a simple estimate of the heating by assuming that the hot electrons are generated at ~ 400 keV and stream into the foil over 1.5 ps (minimum x ray duration measured). Next, assume that we have power dissipation per unit volume of $P = j^2\eta$, where η is the Spitzer resistivity with $\ln\Lambda = 8.7$ and $Z^* = 4$ and j is the current per unit area. If we insist that the resistivity is self-consistent with the plasma temperature reached by the heating then we get $\sim 10-30$ eV, depending on the area we assume ($10-20\ \mu$m to account for spreading of the electrons over a larger area than the focal spot). This level of heating is consistent with experiments by other authors for similar conditions [26] (although with Al targets). However, the Spitzer conductivity is then only $\sim 10^5\ \Omega^{-1}\,\mathrm{m}^{-1}$ and the predicted penetration depth is less than $\sim 1\ \mu$m. This is not consistent with our comparison of thick and thin foils or with the measured ranges of $>200\ \mu$m for the same ~400 keV electron temperature of Pisani *et al.* [27]. We might point out here that recent molecular dynamics simulations [28] indicate that the transition from solid to a plasma may take several picoseconds even for several eV heating: this may affect the validity of assuming Spitzer conductivity—keeping the cold conductivity seems to give better consistency with experiment in this case.

In summary, we have reproduced the peak $K\alpha$ yield well, with simple modeling, without reference to the detailed fast electron dynamics and we might think about why this has been possible with 400 nm irradiance and not with earlier 800 nm data [29]. First, the data above and previous work [26] indicate that electrons do indeed penetrate the thin foil and so range restriction due to electrostatic fields is not a major issue, at least for our metal foils. Also, we are measuring total time and space integrated yields and so as long as we model the number and temperature of the fast electrons realistically and they eventually penetrate into the foil then their detailed orbits should not significantly affect the measurements. One feature that might have affected our ability to model the yield is the issue of recirculating electrons which are not included in the model. The data indicate that they contribute up to ~30% of the signal at tight focus. For the 800 nm case [29] we had a much higher T_{hot} (~1.5 MeV) for the same foil thickness and thus we believe recirculated electrons played a much more significant role and hence the simple modeling failed in that case.

This work was supported by EPSRC Grant No. EP/C001869.

[1] A. Rousse *et al.*, Phys. Rev. E **50**, 2200 (1994).
[2] C. Reich, P. Gibbon, I. Uschmann, and E. Forster, Phys. Rev. Lett. **84**, 4846 (2000).
[3] C. D. Eder, *et al.*, Appl. Phys. B **70**, 211 (2000).
[4] K. B. Wharton, C. D. Boley, A. M. Komashko, A. M. Rubenchik, J. Zweiback, J. Crane, and G. Hays, Phys. Rev. E **64**, 025401(R) (2001).
[5] T. Feurer *et al.*, Phys. Rev. E **65**, 016412 (2001).
[6] D. Salzmann, C. Reich, T. Uschmann, E. Forster, and P. Gibbon, Phys. Rev. E **65**, 036402 (2002).
[7] Ch. Ziener *et al.*, Phys. Rev. E **65**, 066411 (2002).
[8] F. Ewald *et al.*, Europhys. Lett. **60**, 710 (2002).
[9] F. Y. Khattak *et al.*, J. Phys. D **36**, 2372 (2003).
[10] K. B. Wharton *et al.*, Phys. Rev. Lett. **81**, 822 (1998).
[11] M. Hagedorn *et al.*, Appl. Phys. B **77**, 49 (2003).
[12] F. Pisani *et al.*, Appl. Phys. Lett. **84**, 2772 (2004).
[13] H. Nishimura *et al.*, J. Quant. Spectrosc. Radiat. Transf. **81**, 327 (2003).
[14] G. Gregori *et al.*, Contrib. Plasma Phys. **45**, 284 (2005).
[15] M. K. Urry, G. Gregori, O. L. Landen, A. Pak, and S. H. Glenzer, J. Quant. Spectrosc. Radiat. Transf. **99**, 636 (2006).
[16] See, for example, W. L. Kruer, and K. Estabrook, Phys. Fluids **20**, 1688 (1977).
[17] A. R. Bell, J. R. Davies, S. Guerin, and H. Ruhl, Plasma Phys. Controlled Fusion **39**, 653 (1997).
[18] J. R. Davies, A. R. Bell, M. G. Haines, and S. M. Guerin, Phys. Rev. E **56**, 7193 (1997).
[19] P. Gibbon and E. Förster, Plasma Phys. Controlled Fusion **38**, 769 (1996).
[20] D. Riley *et al.*, J. Quant. Spectrosc. Radiat. Transf. **99**, 537 (2006).
[21] F. Brunel, Phys. Rev. Lett. **59**, 52 (1987).
[22] C. A. Quarles, Phys. Rev. A **13**, 1278 (1976).
[23] See, for example, W. E. Burcham, *Elements of Nuclear Physics* (Longman, London, 1979).
[24] F. Brunel, Phys. Fluids **31**, 2714 (1988).
[25] P. Gibbon *et al.*, Phys. Plasmas **6**, 947 (1999).
[26] E. Martinolli *et al.*, Phys. Rev. E **70**, 055402(R) (2004).
[27] F. Pisani *et al.*, Phys. Rev. E **62**, R5927 (2000).
[28] S. Mazevet, J. Clerouin, V. Recoules, P. M. Anglade, and G. Zerah, Phys. Rev. Lett. **95**, 085002 (2005).
[29] D. Riley *et al.*, Phys. Rev. E **71**, 016406 (2005).